Optimality Principles in Variable Stiffness Control: The VSA Hammer

Manolo Garabini[†], Andrea Passaglia[†], Felipe Belo[†], Paolo Salaris[†], and Antonio Bicchi[†‡]

***Abstract*— The control of a robot's mechanical impedance is attracting increasing attention of the robotics community. Recent research in Robotics has recognized the importance of Variable Stiffness Actuators (VSA) in safety and performance of robots. An important step in using VSA for safety has been to understand the optimality principles that regulate the synchronized variation of stiffness and velocity when moving in the shortest time while limiting possible impact forces (the safe brachistochrone problem).**

In this paper, we follow a similar program of understanding the use of VSA in performance enhancement, looking at very dynamic tasks where impacts are maximized. To this purpose we address a new optimization problem that consists in choosing the inputs for maximizing the velocity of a link at a given final position, such as, e.g., for maximizing the effect of a hammer impact. We first study the problem with fixed stiffness, and show that, under realistic modeling assumptions, there does exist an optimal linear spring for the given inertia and motor. We then study optimal control of VSA and show that varying the spring stiffness during the execution of the hammering task improves the final performance substantially. The optimal control law is obtained analytically, thus providing insight in the optimality principles underpinning general VSA control. Finally, we show the practicality of our theoretical results with experimental tests.

I. Introduction

Variable stiffness Actuators (VSA) have been designed to overcome the limits of conventionally actuated robots in terms of safety [1], e.g., in human robot interaction, and for operating in an unstructured environment. After the MIA [2], a device able to slowly adjust its output shaft stiffness, the first prototype able to change stiffness quickly enough to use this capability during a task was the VSA-1 [3]. More recently, actuators with better performances have been developed: the VSA-HD [4], the QA-Joint [5] and the AwAS [6]. During the last years the research community has recognized the importance of compliant actuators in the context of optimization problems. First, the optimal control problem of performing a rest to rest position task under a safety constraint in minimum time is solved in [1] (namely the *safe brachistochrone* problem). This solution shows that the VSAs achieve better performance with respect to conventional actuators and to Series Elastic Actuators (SEAs). This improvement is significant when the link and end effector inertia are small, as described in [7] and [8]. However, the true potential of performance improvement embedded in variable stiffness actuation is still to be explored, as suggested by examples in nature. The capability of soft actuators (e.g., SEAs) to achieve higher speeds than those of standard motors has been shown in [9], [10], [11], and [12]. The usage of VSAs in maximizing energy efficiency has been investigated in [13] and in [14]. Some possible applications of speed optimization using VSAs are throwing objects, kicking a ball as a soccer player, or hammering a nail. Work in this direction, although in a different setting than what described below, will be reported in [15].

In this paper we address the problem of maximizing link speed at a given position for both constant and variable stiffness actuators (SEA and VSA, respectively) through the application of optimal control theory.

We first present analytical solutions for three SEA cases, considering as control input reference position, speed, and acceleration, respectively. The three cases, considered separately, illustrate diverging motivations for the optimal stiffness choice. However, in a realistic setting where the different aspects are merged, we show that an optimal (constant) stiffness exists for any given inertia and motor torque.

We then study optimal control of VSA and present analytical results illustrating the optimal synchronization of the spring equilibrium position and stiffness variations. We show that varying the stiffness during the execution of the hammering task improves the final performance substantially (a formula for quantifying the improvement is provided). To demonstrate the realism of assumptions made in the problem setup, and the practical applicability of the obtained control laws, we finally provide experimental results confirming our theoretical predictions.

II. Problem Definition

In this paper we investigate different optimal control problems which dynamics is always represented by the simplest model of a compliant actuator link system:

$$\ddot{q}+\omega^2(q-\theta)=0\,, \tag{1}$$

where $\omega=\sqrt{k/m}$ and the other variables are defined in Fig. 1. Given a state-form $\dot{x}=f(x,u)$, and the initial condition $x(0)=0$, our problems mainly differ in the way system state $x(t)\in\mathbb{R}^n$ and system inputs $u(t)\in U\subset\mathbb{R}^m$ are defined. Table I shows the SEA problems studied, and table II describes the VSA problem studied. As our goal is always

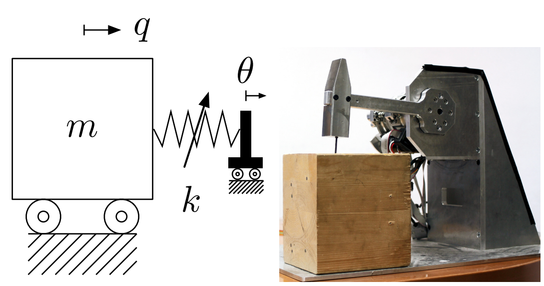

(a) (b)

Fig. 1. (a)Scheme of a compliant actuator, where k denotes the spring stiffness, m the link (hammer) inertia, q the link position and θ the rotor position. (b)Picture of the experimental setup

[†] Interdepart. Research Center "E. Piaggio", University of Pisa, Via Diotisalvi, 2, 56100 Pisa, Italy.

[‡] Department of Advanced Robotics, Istituto Italiano di Tecnologia, via Morego, 30, 16163 Genova

that of maximizing the link speed at the final instant T, we define the performance index

$$J = \phi(x(T)) = x_2(T) = \dot{q}(T)\,. \tag{2}$$

Without lack of generalization, the final position constraint is defined as

$$\psi(x(T)) = x_1(T) = q(T) = 0\,. \tag{3}$$

The Hamiltonian function is thus reduced to

$$H(x(t), \lambda(t), u(t)) = \lambda^T(t) f(x(t), u(t))\,, \tag{4}$$

where $\lambda(t) \in \mathbb{R}^n$ is the vector of the adjoint variables. From the optimal control theory [16], the necessary conditions to optimize the performance index are:

$$\dot{\lambda}^T(t) = -\frac{\partial H(x(t), u(t))}{\partial x(t)} \tag{5}$$

$$\lambda^T(T) = \frac{\partial \phi(x(T))}{\partial x(T)} + \nu \frac{\partial \psi(x(T))}{\partial x(T)} = [\nu, 1, 0, \ldots, 0]\,. \tag{6}$$

Given that we are studying autonomous systems without state path constraints, the Hamiltonian is constant. Moreover, in unspecified terminal time problems where $\partial_T \phi(x(T)) = 0$ and $\partial_T \psi(x(T)) = 0$, we have the further necessary condition $H(x(t), \lambda(t), u(t))|_{t=T} = 0$, hence we can conclude that:

$$H(x(t), \lambda(t), u(t)) = 0 \quad \forall t \in [0, T]\,. \tag{7}$$

The control domain U is defined as

$$U = \{u : u_{min} < u < u_{max}\}\,, \tag{8}$$

where u_{min} and u_{max} are the vectors of achievable minimum and maximum input values.

Finally, in order to determine the optimal solutions, the Hamiltonian is maximized along u according to the Maximum Principle [16].

III. Optimal Control: SEA

In section III-A we investigate the speed optimization of SEAs, [17], without considering path constraints. These are considered in section III-B.

A. Models without state path constraints

We tackle the problem considering the following variables as input controls: equilibrium position (P), speed (S), and acceleration (A). Table I summarizes the most relevant equations to properly expose the adopted method, as described in section II. In the first row we present the state space definition of each case. Instead of (8) we can use a simpler inequality constraint: $|u| \le u_{max}$. The second and the third rows present the Hamiltonian functions, as defined in (4), and the co-state dynamics, as defined in (5), respectively. The optimal control laws derived with the Maximum Principle are reported in the fourth row. The switching functions $\lambda_n(t)$ as a function of $\nu(T)$ can be obtained through the solution of the co-state dynamics. By applying the condition (7) in $t = 0$ and by substituting the state initial conditions we can determine the switching function initial condition:

$$\lambda_n(t)|_{t=0} = 0\,. \tag{9}$$

By solving the co-state final values problem and by exploiting (9) we obtain $\nu(T)$ as reported in the fifth row of the table I.

We decided to analyze the problem considering one switching only as done by humans when they use their limbs to dash an object, i.e., a soccer ball or to hammer a nail. E.g., during a hammering task, humans change the arm movement direction only once. We assume that the control value in the first piece is $-u_{max}$ while the second one is u_{max} (this assumption is proved in section IV). The solution of the system of differential equations $\dot{x} = f(x, u)$ permits us to derive $x(t)$ for the intervals $t \in [0, t_1)$ and $t \in (t_1, T]$. Now we can apply the final state constraint (3) to determine the implicit relationship

$$x_1(t_1, t)|_{t=T} = 0\,. \tag{10}$$

We can also write a second implicit relationship that is determined in correspondence of a zero crossing of the switching function at switching time $t = t_1$:

$$\lambda_n(t)|_{t=t_1} = 0\,. \tag{11}$$

At this moment both (10) and (11) are functions of the system parameters and the unknowns are t_1 and t_2 only. If we consider the suitable change of coordinates

$$T = t_1 + t_2\,, \quad t_1 = \frac{c_1}{\omega}, \quad t_2 = \frac{c_2}{\omega}, \tag{12}$$

then (10) together with (11) compose a system of two equations and two unknowns, constants c_1 and c_2, as reported in sixth row of table I. Note that these constants do not depend on system parameters and can be determined analytically or numerically (results are reported in table I). Finally t_1 and t_2 can be obtained from (12) and the link hit speed can be easily evaluated from the solution of $x(t)$ as reported in table I.

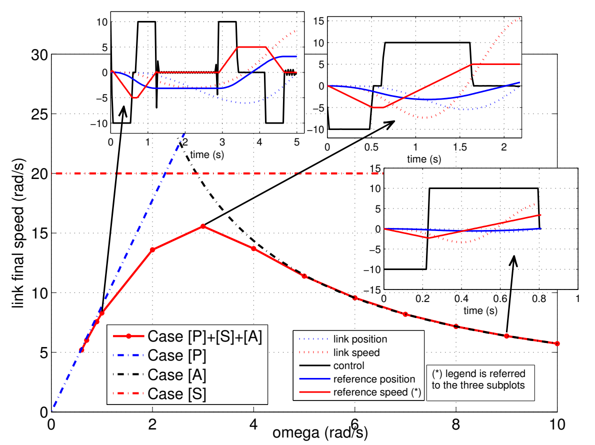

Fig. 2. V_{max} and hit time T vs ω for cases (P), (S) and (A). The continuous line shows the behavior of case (A) with boundaries on θ_{max} and $\dot{\theta}_{max}$.

B. Constrained model

From the results obtained we can verify that when only θ is constrained then final speed is proportional to the parameter ω, when only $\dot{\theta}$ is constrained the final speed does not depend on ω and when only $\ddot{\theta}$ is constrained the final speed is inversely proportional to ω. We conclude that a realistic analysis of the influence of ω on the final achievable speed must consider state path constraints on θ, $\dot{\theta}$, $\ddot{\theta}$ concurrently. Thus, in this section we review problem (A)

	Position control (P)	Speed control (S)	Acceleration control (A)
State space definition	$\begin{cases} x^T = [q \quad \dot{q}] \\ u = \theta \\ \dot{x} = \begin{bmatrix} x_2 \\ \omega^2 (u - x_1) \end{bmatrix} \end{cases}$	$\begin{cases} x^T = [q \quad \dot{q} \quad \theta] \\ u = \dot{\theta} \\ \dot{x} = \begin{bmatrix} x_2 \\ \omega^2 (x_3 - x_1) \\ u \end{bmatrix} \end{cases}$	$\begin{cases} x^T = [q \quad \dot{q} \quad \theta \quad \dot{\theta}] \\ u = \ddot{\theta} \\ \dot{x} = \begin{bmatrix} x_2 \\ \omega^2 (x_3 - x_1) \\ x_4 \\ u \end{bmatrix} \end{cases}$
Hamiltonian	$H = \lambda_1 x_2 + \lambda_2 \omega^2 (u - x_1)$	$H = \lambda_1 x_2 + \lambda_2 \omega^2 (x_3 - x_1) + \lambda_3 u$	$H = \lambda_1 x_2 + \lambda_2 \omega^2 (x_3 - x_1) + \lambda_3 x_4 + \lambda_4 u$
Co-state dynamics	$\dot{\lambda}^T = [\omega^2 \lambda_2 \quad -\lambda_1]$	$\dot{\lambda}^T = [\omega^2 \lambda_2 \quad -\lambda_1 \quad -\omega^2 \lambda_2]$	$\dot{\lambda}^T = [\omega^2 \lambda_2 \quad -\lambda_1 \quad -\omega^2 \lambda_2 \quad -\lambda_3]$
Optimal control law	$u^* = u_{max} \text{sign}(\lambda_2)$	$u^* = u_{max} \text{sign}(\lambda_3)$	$u^* = u_{max} \text{sign}(\lambda_4)$
Switching function	$\lambda_2 = \cos((T-t)\omega) + \frac{\nu \sin((T-t)\omega)}{\omega}$ $\nu = -\omega \cot(T\omega)$	$\lambda_3 = \nu - \nu \cos((T-t)\omega) + \omega \sin((T-t)\omega)$ $\nu = \frac{\omega \sin(T\omega)}{\cos(T\omega) - 1}$	$\lambda_4 = 1 + T\nu - t\nu - \cos((T-t)\omega) - \frac{\nu \sin((T-t)\omega)}{\omega}$ $\nu = \frac{\omega(-1 + \cos(T\omega))}{T\omega - \sin(T)}$
Switching constants	$\begin{cases} 1 - 2\cos(c_2) + \cos(c_2 + c_1) = 0 \\ \csc(c_1 + c_2)\sin(c_1) = 0 \end{cases}$ $c_1 = \pi, \quad c_2 = 2\arctan\left(\frac{1}{\sqrt{2}}\right)$	$\begin{cases} c_2 - c_1 - 2\sin(c_2) + \sin(c_2 + c_1) = 0 \\ \sin(c_2) + \frac{\sin(c_1+c_2)}{-1+\cos(c_1+c_2)} - \frac{\cos(c_2)\sin(c_1+c_2)}{-1+\cos(c_1+c_2)} = 0 \end{cases}$ $c_1 = \pi, \quad c_2 = \pi$	$\begin{cases} 2 + c_1^2 + 2c_1 c_2 - c_2^2 - 4\cos(c_2) + 2\cos(c_1 + c_2) = 0 \\ c_1 - (c_1 + c_2)\cos(c_2) + c_2 \cos(c_1 + c_2) + \sin(c_1) + \sin(c_2) - \sin(c_1 + c_2) = 0 \end{cases}$ $c_1 \approx 2.11, \quad c_2 \approx 5.24\pi$
Link final speed	$v_{max} = 2\sqrt{2} u_{max} \omega$	$v_{max} = 4 u_{max}$	$v_{max} = 5.74 \frac{u_{max}}{\omega}$

TABLE I

ANALYTICALLY SOLVED OPTIMAL CONTROL PROBLEMS FOR SEA.

with the further state constraints, $|x_3| < \theta_{max}$ and $|x_4| < \dot{\theta}_{max}$, where $\dot{\theta}_{max}$ and θ_{max} represent the maximum motor speed and position respectively. We postpone an analytical analysis of this problem to future work and discuss results on the basis of numerical solutions obtained using the tool ACADO© [18]. The influence of ω on the final speed is shown in Fig. 2 together with the theoretical maximum speeds w.r.t. the problems (P), (S) and (A). It is observed that when position and speed constraints are not active, then system behaves as model (A) (right region of the plot); when the speed constraint is prevalent, then system behaves as model (S) (middle region of the plot); and, when the position constraint is predominant, then system behaves as model (P) (left region of the plot); We thus understand that, given a link inertia, there exists an optimal value of the spring stiffness that maximizes the final achievable speed.

IV. OPTIMAL CONTROL: VSA

The considerations made so far lead us to think that the exploitation of stiffness by a VSA may permit us to work near the optimal speed region (see Fig. 2) even for different link inertia. Indeed, we will see that the possibility of adjusting stiffness during the task gives further advantages w.r.t. the SEA case. Thus, in this section we investigate the VSA problem where system inputs are defined as the spring stiffness k and equilibrium position θ.

Table II summarizes the most relevant equation to properly expose the adopted method to analyze the problem, similarly to section III. According to (8) $u_{min}^T = [-u_{1,max} \quad u_{2,min}] = [-\theta_{max} \quad k_{min}]$ and $u_{max}^T = [u_{1,max} \quad u_{2,max}] = [\theta_{max} \quad k_{max}]$, where $k_{max} > k_{min} > 0$ and $\theta_{max} > 0$. In this section we first approach the problem without considering the final position constraint, then we discuss in remark 5 that by shifting the control constraints, the resulting optimal control laws can also be adopted in order to respect a terminal position constraint.

By evaluating $\partial_u H = 0$ we can conclude that u^* must belong to the boundaries of its domain, and we can obtain the switching conditions of u^*, reported in the fourth row of table II, by maximizing the Hamiltonian. The optimal control is a bang-bang control. In the following we present all considerations that allow us to construct the optimal switching sequence.

Remark 1: Given that u_1 and u_2 are constant between two switching instants, t' and t'', the solutions of state and co-state dynamics (first and third row of table II) for $t \in [t', t'']$ are:

$$\begin{bmatrix} x_1(t) \\ x_2(t) \\ \lambda_1(t) \\ \lambda_2(t) \end{bmatrix} = \begin{bmatrix} u_1 + (\bar{x}_1 - u_1)\cos(\omega_{u_2}\Delta t) + \omega_{u_2}^{-1}\bar{x}_2 \sin(\omega_{u_2}\Delta t) \\ \bar{x}_2 \cos(\omega_{u_2}\Delta t) + \omega_{u_2}(u_1 - \bar{x}_1)\sin(\omega_{u_2}\Delta t) \\ \bar{\lambda}_1 \cos(\omega_{u_2}\Delta t) + \omega_{u_2}\bar{\lambda}_2 \sin(\omega_{u_2}\Delta t) \\ \bar{\lambda}_2 \cos(\omega_{u_2}\Delta t) - \omega_{u_2}^{-1}\bar{\lambda}_1 \sin(\omega_{u_2}\Delta t) \end{bmatrix} \quad (13)$$

where $\omega_{u_2} = \sqrt{u_2/m}$ is the common frequency of all solutions, $\bar{x}_1 = x_1(t')$, $\bar{x}_2 = x_2(t')$, $\bar{\lambda}_1 = \lambda_1(t')$ and $\bar{\lambda}_2 = \lambda_2(t')$ are the initial conditions and $\Delta t = t - t'$. Moreover all the functions are continuous piecewise.

Symbol S_2 denotes a switching where u_2^* goes from k_{max} to k_{min} while $S_{1,2}$ denotes a switching where u_2^* goes from k_{min} to k_{max} and u_1^* changes.

State space definition	$\begin{cases} x^T = [q \quad \dot{q}] \\ u^T = [\theta \quad k] \\ \dot{x} = \begin{bmatrix} x_2 \\ \frac{u_2}{m}(u_1 - x_1) \end{bmatrix} \end{cases}$
Hamiltonian	$H = \lambda_1 x_2 - \lambda_2 \frac{u_2}{m}(x_1 - u_1)$
Co-State dynamics	$\begin{cases} \dot{\lambda}^T = \begin{bmatrix} \frac{u_2}{m}\lambda_2 & -\lambda_1 \end{bmatrix} \\ \lambda(T)^T = [0 \quad 1] \end{cases}$
Optimal control law	$u_1^* = \begin{cases} u_{1,max} \text{ if } \lambda_2 > 0 \\ -u_{1,max} \text{ if } \lambda_2 < 0 \end{cases}$ $u_2^* = \begin{cases} u_{2,max} \text{ if } \lambda_2 (u_1 - x_1) > 0 \\ u_{2,min} \text{ if } \lambda_2 (u_1 - x_1) < 0 \end{cases}$

TABLE II
ANALYTICALLY SOLVED OPTIMAL CONTROL PROBLEMS FOR VSA. THE LACK OF THE LAST THREE ROWS SHOWN IN TABLE I IS DUE TO THE DIFFERENT WAY TO OBTAIN THE SOLUTIONS.

Theorem 1: The optimal control is characterized by the following properties:

1) the switching sequence is

$$\{S_2; S_{1,2}; S_2; \ldots; S_2; S_{1,2}\}\,, \tag{14}$$

2) the time between S_2 and $S_{1,2}$ is

$$t_{S_{1,2}} = \sqrt{m/k_{min}}\pi/2\,, \tag{15}$$

3) the time between $S_{1,2}$ and S_2, the time of the first period and the time of the last period are:

$$t_{S_2} = \sqrt{m/k_{max}}\pi/2\,, \tag{16}$$

To prove theorem 1 we must present some preliminary results. The proof of the theorem is a direct consequence of the following propositions presented in this section. These propositions are also complimentary in order to have a complete understanding of the optimal control scheme.

Proposition 1: The optimal control u_2^* at initial time is $k_{\max}$.

Proof: From the optimal control law, we have that the value of $u_2^*|_{t=0}$ depends on $\text{sign}(\lambda_2(u_1 - x_1))|_{t=0}$ and that $\text{sign}(\lambda_2) = \text{sign}(u_1)$. Given that $x_1|_{t=0} = 0$, then $\lambda_2 u_1|_{t=0} \geq 0$. Hence, we have the thesis. ■

Proposition 2: The first switching is S_2 and it occurs at time (16) when the speed is piecewise maximum.

Proof: Equation (7) evaluated in $t = 0$ gives $\lambda_2|_{t=0} = 0$. Consider (13) with $\bar{\lambda}_2 = \lambda_2|_{t=0}$, $\bar{x}_2 = 0$ and, by proposition 1, $u_2 = k_{max}$. Since λ_2 and $u_1 - x_1$ are continuous for $t \in [0, t_1'']$, we can find the two possible switching times by imposing $\lambda_2(t_1'') = 0$ and $|u_{1,max} - x_1(t_1'')| = 0$. The latter condition gives the smallest time,i.e., (16). By substituting $|u_{1,max} - x_1(t_1'')| = 0$ in the state dynamics, reported in table II, it follows that $\ddot{q}|_{t=t_{S_2}} = 0$. Hence we have the thesis. ■

Proposition 3: The second switching is $S_{1,2}$ and the time between the first switching S_2 and the second switching $S_{1,2}$ is given by (15).

Proof: By substituting $\bar{\lambda}_2 = \lambda_2|_{t=0}$, $\bar{x}_2 = 0$, $u_2 = k_{max}$ in (13) and by evaluating $|x(t_{S_2})|$ we obtain:

$$|x_1(t_{S_2}) - u_{1,max}| = 0 \tag{17}$$
$$|x_2(t_{S_2})| = u_{1,max}\omega_{u_{2,max}}\,. \tag{18}$$

By evaluating (7) at $t = t_{S_2}$ it follows that $\lambda_1|_{t=t_{S_2}} = 0$. Since S_2 occurs at t_{S_2}, by substituting $\bar{x}_1 = u_{1,max}$, $\bar{\lambda}_1 = \lambda_1|_{t=t_{S_2}} = 0$, $u_2 = k_{min}$ in (13) we obtain $x(t)$ and $\lambda(t)$ for $t \in [t_{S_2}, t_2'']$. Since they are continuous we determine $t_{S_{1,2}} = t_2'' - t_{u_2}$ as the smallest time between the switchings that can be found by imposing the conditions $|x_1 - u_1||_{t=t_{S_{1,2}}} = 0$ and $\lambda_2|_{t=t_{S_{1,2}}} = 0$. The latter condition gives the smallest time, i.e., (15). By evaluating $|x(t_{S_{1,2}})|$ at the instant of the second switching it follows that:

$$\begin{aligned} |x_1 - u_1||_{t=t_{S_{1,2}}} &= |x_1 - u_1||_{t=0}\sqrt{(k_{max}/k_{min})} \\ &= u_{1,max}\sqrt{(k_{max}/k_{min})} \end{aligned} \tag{19}$$
$$x_2|_{t=t_{S_{1,2}}} = 0 \tag{20}$$

Since $\sqrt{(k_{max}/k_{min})} > 1$, then the $\text{sign}(u_1 - x_1)$ does not change. Consequently, u_2 changes to k_{max} because the sign of λ_2 changes (as can be verified in table II). Hence we obtain the thesis. ■

Remark 2: The proofs of propositions 2 and 3 are independent of the sign of u_1.

Proposition 4: The optimal switchings alternate between S_2 and $S_{1,2}$. The time between S_2 and $S_{1,2}$ is given by (15), while the time between $S_{1,2}$ and a S_2 is given by (16).

Proof: By imposing (7) in $t = t_{S_{1,2}}$ it follows that $\lambda_2|_{t=t_{S_{1,2}}} = 0$. Given (20), $u_2 = k_{max}$ for $t \geq t_2''$ and by proposition 3, we return to the starting conditions:

$$x_2|_{t=t_{S_{1,2}}} = x_2|_{t=0} \tag{21}$$
$$\lambda_2|_{t=t_{S_{1,2}}} = \lambda_2|_{t=0} = 0 \tag{22}$$
$$u_2|_{t>t_{S_{1,2}}} = u_2|_{t>0} = k_{max} \tag{23}$$

Propositions 2 and 3 still hold, and by using logical induction it can be shown that they can be applied recursively. Hence we obtain the thesis. ■

Proposition 5: At the final time $t = T$, the optimal control is $[u_1^*(T) = \theta_{\max} \quad u_2^*(T) = k_{\max}]$

Proof: The control $u_1^*(T) = \theta_{\max}$ comes from $\lambda_2(T) = 1$. We prove that $u_2(T) = k_{max}$ by contradiction. Assume that the control u^* is optimal and $u_2^*(T) = k_{min}$. We have from theorem 4 that the last switching is S_2 and we consider that it happened at $t_l = T - \Delta t$. By propositions 2 and 4 we have that $x_2(t_l) = \hat{x}_2$ is maximum on the last interval in which u_1 is constant. Now, if we choose the alternative control

$$u^\#(t) = \begin{cases} 0 & \text{if } t < \Delta\text{t} \\ u^*(t - \Delta\text{t}) & \text{if } t > \Delta\text{t} \end{cases},$$

it would have reached the maximum velocity $x_2(T, u^\#) = \hat{x}_2$ with maximum stiffness $u_2(T)^\# = k_{max}$. Given that $x_2(T, u^\#) > x_2(T, u^*)$, the impossibility is proved. ■

Remark 3: The number N must be even. This is verified by contradiction: if N is odd, then u_2 at initial time does not respect proposition 1. We can also observe that if $N/2$ is odd $u_1|_{t=0} = -u_{1,max}$, otherwise $u_1|_{t=0} = u_{1,max}$.

Remark 4: If follows from theorem 1 that:

$$T = \frac{\pi\sqrt{m}}{2}\left(\frac{N\left(\sqrt{k_{\max}}+\sqrt{k_{\min}}\right)}{2\sqrt{k_{\min}k_{\max}}}+\frac{1}{\sqrt{k_{\max}}}\right). \quad (24)$$

Remark 5: If $-2u_{1,max} \leq u \leq 0$, then the presented solution corresponds to that of final constraint $x_1(T) = 0$. This is easy to verify as follows. When the maximum speed occurs, $\ddot{q} = 0$ and, consequently, $x_1 = u_1$ (please check table II), i.e., the entire energy of the system is kinetic and elastic energy stored in the spring must be zero. Therefore, at final time, $x_1(T) = u_{1,max}$. If we shift the control contraints to $-2u_{1,max} \leq u \leq 0$, the theorem 1 still holds, and the presented solution corresponds to that of final constraint $x_1(T) = 0$. Moreover, it should be noticed that, fixed $\delta_u = u_{1,max} - u_{1,min}$, by shifting the control bounds as described, it is possible to obtain the highest terminal speed, since at the beginning we can stretch the spring with the maximum allowed deformation δ, such to store in the system the maximum initial potential energy.

In order to compare maximum speeds obtained when using a SEA (v_{SEA}) and when using a VSA (v_{VSA}) after a single switching of the equilibrium position, we have that the final speed after a single switching case is

$$v = 2u_{1,max}\sqrt{k_{max}/m}\left(1+(k_{max}/k_{min})^{1/2}\right). \quad (25)$$

and consequently:

$$\frac{v_{VSA}}{v_{SEA}} = \frac{1+(k_{max}/k_{min})^{1/2}}{2}. \quad (26)$$

E.g., by assuming $k_{min} = 0.5k_{max}$ it is $v_{VSA}/v_{SEA} \approx 1.2$. Note that the comparison bewteen VSA speed and SEA speed is performed considering the problem with control boundary shifted to $[-2u_{max}, 0]$ in both cases (the SEA speed can be derived by imposing $k_{min} = k_{max}$ in (25)). Note also that in section III the problem (P) was discussed without considering this bounds' shifting in order to maintain an uniform presentation of the three cases studied.

We thus conclude that the exploitation of stiffness during the task, improves the performance of the system. Nevertheless we should notice that this model, useful to understand the optimal control strategy, is not very reliable when k_{max} becomes too high for the same reasons reported in section III. The fact that we neglect the dynamics of the stiffness is subject to the same considerations. Moreover, we implicitly admit that the actuator's prime movers and the elastic transmission work within a feasible range, and that the achievable stiffness range does not depend on the link and equilibrium positions. Obtained results confirm that with a VSA we can improve the performance of a SEA.

Theorem 2: The stiffness optimal control is:

$$u_2 = \begin{cases} u_{2,\max} & \text{if } \dot{q}\ddot{q} > 0 \\ u_{2,\min} & \text{if } \dot{q}\ddot{q} < 0 \end{cases} \quad (27)$$

Proof: From proposition 3 we have that when a $S_{1,2}$ switching occurs it is $\dot{q} = 0$. From proposition 2 we have that when a S_2 switching occurs it is $\ddot{q} = 0$. Hence, when a stiffness switching occurs it is $\dot{q}\ddot{q} = 0$.

From proposition 1 we have that $u_2|_{t=t_0} = u_{2,\max}$. Moreover, given that at initial state $\dot{q}|_{t=t_0} = 0, \ddot{q}|_{t=t_0} = 0$ then $\dot{q}\ddot{q} > 0|_{t=t_0^+}$.

Hence, as $\dot{q}\ddot{q}$ is a continuous function, we have the thesis. ■

V. EXPERIMENTAL RESULTS

case	type	inertia	boundary	$\dot{q}(T)$
(a)	SEA-like	$m = 0.1$kg	$q_{D,max}$	$\simeq 207$deg/s
(b)	SEA-like	$m = 0.1$kg	$q_{D,min}$	$\simeq 242$deg/s
(c)	VSA	$m = 0.1$kg	$q_{S,min,max}$	$\simeq 276$deg/s
(d)	SEA-like	$m = 1$kg	$q_{D,max}$	$\simeq 341$deg/s
(e)	SEA-like	$m = 1$kg	$q_{D,mid}$	$\simeq 374$deg/s
(f)	VSA	$m = 1$kg	$q_{S,min,max}$	$\simeq 499$deg/s

TABLE III

FIRST AND SECOND COLUMNS DEAL WITH THE SIX EXPERIMENTS' CASES. THE THIRD AND THE FOURTH SHOW THE FIXED PARAMETERS. FINALLY, IN THE FIFTH COLUMN ARE SHOWN THE MEASURED VALUES OF LINK SPEED AT HIT TIME

A. Experimental Setup

The experimental setup comprises one VSA-Cube, a low cost prototype of a bidirectional antagonistic VSA developed by Centro Piaggio [19], connected to a Simulink interface through an I^2C bus. We mounted two different weights at the edge of the link, which length is 0.15 m. Control inputs are $q_S = \frac{q_1+q_2}{2}$ and $q_D = \frac{q_1-q_2}{2}$, where $q_{1,2}$ are the two motor angles, q_S and q_D are the output shaft position and stiffness preset, respectively. An encoder embedded on the actuator reads the link position. By deriving the properly-filtered link position it is possible to obtain link speed.

B. Experimental results

Three experiments were conducted for each mass: in the first one we implemented the optimal control scheme; in the second one we switch only the equilibrium position while keeping the preset constant at its minimum value; and, in the last one, we keep the preset at its maximum value.

Figure 3 and table III show a summary of the experimental results. It is observed that the first experiment is, indeed, the one that produces the best results. The experiment conducted with low stiffness preset presents better performance than that with high stiffness preset. We believe that this result is a consequence of the springs' nonlinearity, i.e., the fact that stiffness does not remain constant during the whole experiment. The experimental values of switching times are larger than the theoretically evaluated ones because of the time delays in real system, the limited speed of the VSA-Cube prime movers, and the inability to precisely align the stiffness with the given q_D control.

VI. CONCLUSION AND FUTURE WORK

In this paper we tackle the problem of maximizing link velocity at an unspecified terminal time when using SEAs and VSAs and we compare their performance. Analytical results showed that a SEA performing a hammering task can reach a speed up to four times that of the actuator's prime mover when using one equilibrium position switching. We also show that when position, speed and acceleration constraints are considered, there exists an optimal spring that maximizes the final speed for a given link inertia.

Then, we presented an analytical solution for the VSA case and we demonstrate that the theoretical SEA speed limit can be significantly overcame by a VSA. Experiments confirm that when adjusting the stiffness during the task it is possible to obtain better performances than using a SEA. We obtained a speed increase of up to 30% using a VSA.

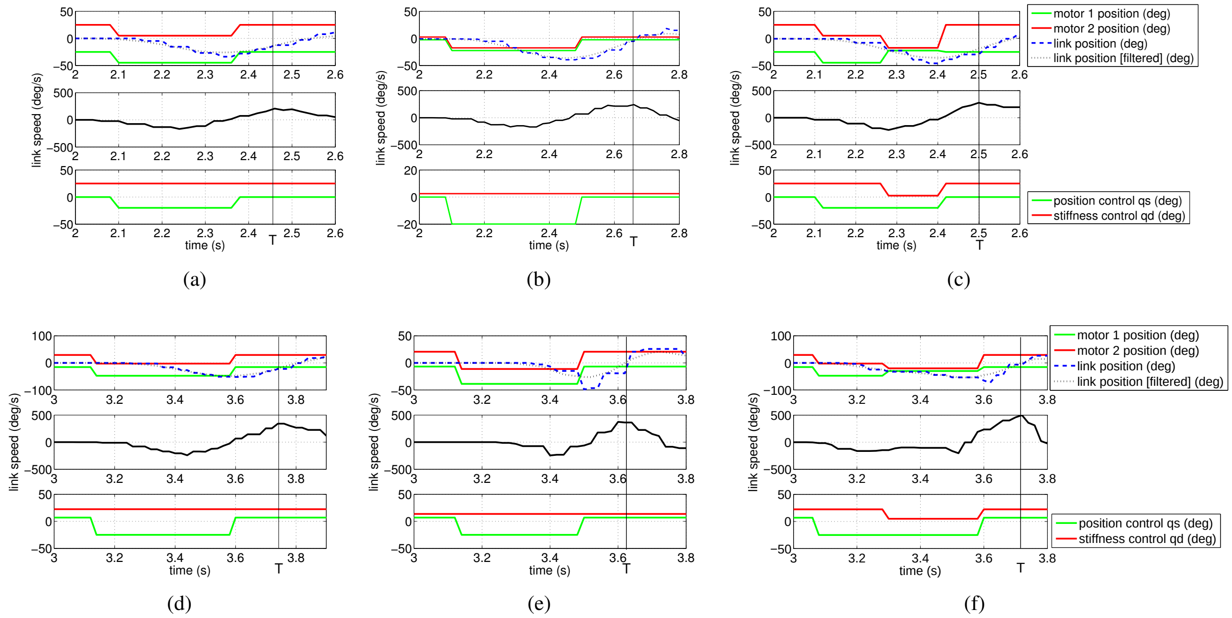

Fig. 3. Summary of the experimental results obtained with the VSA-Cube. The two lines are referred to two different masses mounted on the link. In first column the stiffness preset q_D, defined in [19], is fixed to the maximum value, while in the second column it's fixed to the medium or the minimum values. In the third column q_D is an optimized input. Input's boundary values are $q_{D,min} = 5$deg, $q_{D,max} = 50$deg, $q_{S,min} = -20$deg and $q_{S,max} = 0$deg.

A. Future Work

We have investigated the analysis of more complex models via numerical tools, obtained results will be shown in future work. We have also already observed that in some cases it is possible to obtain a good performance with a system like a SEA with a nonlinear spring of suited shape. The study of these devices is left for future work.

VII. Acknowledgments

The authors gratefully acknowledge the contribution of Manuel Catalano, Giorgio Grioli, Fabio Bonomo, Michele Mancini, Andrea Di Basco and Fabio Vivaldi.

The research leading to these results has received funding from the European Community's Seventh Framework Programme (FP7/2007-2013) under grant agreements n IST-231554-2008 (VIACTORS), and n ICT-248587-2010 (THE).

References

[1] A. Bicchi and G. Tonietti, "Fast and soft arm tactics: Dealing with the safety-performance tradeoff in robot arms design and control," *IEEE Robotics and Automation Magazine*, vol. 11, no. 2, June 2004.

[2] T. Morito and S. Sugano, "Development and evaluation of seven-d.o.f. mia arm," *IEEE Int. Conf on Robotics and Automation*, pp. 462–267, April 1997.

[3] G. Tonietti, R. Schiavi, and A. Bicchi, "Design and control of a variable stiffness actuator for safe and fast physical human/robot interaction," *IEEE Int. Conf. on Robotics and Automation*, pp. 526–531, April 2005.

[4] M. G. Catalano, G. Grioli, F. Bonomo, R. Schiavi, and A. Bicchi, "Vsa-hd: From the enumeration analysis to the prototypical implementation," *IEEE/RSJ Int.Conf. on Intelligent Robots and Systems*, pp. 3676–3681, 2010.

[5] O. Eiberger, S. Haddadin, M. Weis, A. Albu-Schaffer, and G. Hirzinger, "On joint design with intrinsic variable compliance: Derivation of the dlr qa-joint," *IEEE Int. Conf. on Robotics and Automation*, pp. 1681–1694, 2010.

[6] A. Jafari, N. G. Tsagarakis, B. Vanderborght, and D. G. Caldwell, "A novel actuator with adjustable stiffness (awas)," *IEEE/RSJ Int. Conf. on Intelligent Robots and Systems*, pp. 4201–4206, 2010.

[7] S. Haddadin, A. Albu-Schaffer, O. Eiberger, and G. Hirzinger, "New insights concerning intrinsic joint elasticity for safety," *IEEE/RSJ Int. Conf. on Intelligent Robots and Systems*, pp. 2182–2187, 2010.

[8] S. Haddadin, A. Albu-Schaffer, and G. Hirzinger, "The role of the robot mass and velocity in physical human-robot interaction - part i: Non-constrained blunt impacts," *IEEE Int. Conf. on Robotics and Automation*, pp. 1331–1338, 2008.

[9] H. Schempf, C. Kraeuter, and M. Blackwell, "Roboleg: A robotic soccer-ball kicking leg," *IEEE Int. Conf. on Robotics and Automation*, vol. 2, pp. 1314–1318, 1995.

[10] D. Paluska and H. Herr, "The effect of series elasticity on actuator power and work output: Implications for robotic and prosthetic joint design," *Robotics and Autonomous Systems*, vol. 54, pp. 667–673, 2006.

[11] M. Okada, S. Ban, and Y. Nakamura, "Skill of compliance with controlled charging/discharging of kinetic energy," *IEEE Int. Conf. on Robotics and Automation*, pp. 2455–2460, 2002.

[12] S. Wolf and G. Hirzinger, "A new variable stiffness design: Matching requirements of the next robot generation," *IEEE Int. Conf. on Robotics and Automation*, pp. 1741–1746, 2008.

[13] J. Yamaguchi, S. Inoue, D. Nishino, and A. Takanishi, "Development of a bipedal humanoid robot having antagonistic driven joints and three dof trunk," *IEEE/RSJ Int. Conf. on Intelligent Robots and Systems*, pp. 96–101, 1998.

[14] B. Vanderborght, B. Verrelst, R. V. Ham, M. V. Damme, D. Lefeber, B. Duran, and P. Beyl, "Exploiting natural dynamics to reduce energy consumption by controlling the compliance of soft actuators," *Int. Journal of Robotics Research,*, vol. 25, no. 4, pp. 343–358, 2006.

[15] S. Haddadin, M. Weis, S. Wolf, and A. Albu-Schaffer, "Optimal control for maximmizing link velocity of robotic variable stiffness joints," 2011, (in press) IFAC WC.

[16] A. Bryson and Y. Ho, *Applied Optimal Control*. Taylor & Francis, 1975.

[17] G. A. Pratt and M. Williamson, "Series elastic actuators," *IEEE/RSJ Int. Conf. on Intelligent Robots and Systems*, pp. 399–406, 1995.

[18] D. Ariens, B. Houksa, H. Ferreau, and F. Logist, *ACADO for Matlab User's Manual*, Optimization in Engineering Center (OPTEC), http://www.acadotoolkit.org/, May 2010.

[19] M. G. Catalano, G. Grioli, M. Garabini, F. Bonomo, M. Mancini, N. Tsagarakis, and A. Bicchi, "Vsa - cubebot. a modular variable stiffness platform for multi degrees of freedom systems," in *IEEE Int. Conf. on Robotics and Automation*, 2011.